Starting Performance Analysis of Single-Phase Capacitor Motor Using Finite Element Method

Krikor S. Krikor* **Dhari Y. Mahmood*** **Maha K. Yousif***

Received on : 16/102007
Accepted On: 3/1/2008

Abstract

This paper presents the starting performance analysis of the single-phase capacitor motor and the effect of motor capacitor on the starting performance. The analysis approach is based on 2-D finite element method for the transient case, with the software (ANSYS V.8). The validity of the proposed analysis method is verified by experimental values which are found to be in good agreement.

Keywords : Single-phase capacitor motor, finite element analysis, circuit couple.

الخلاصة

يعرض البحث الحالي تحليل خصائص بدء محرك المتسعة أحادي الطور وتأثير متسـعة المحـرك على خصائص البدء. التحليل مبني على أساس طريقة العنصر المحدد ثنائي الأبعاد للحالـة العـابرة وذلـك باستخدام برمجيات (ANSYS) الجزء 8. للتحقق من صحة الطريقة المقترحة للتحليل تم مقارنة النتائج مع تلك المستحصلة عمليا وكانت النتائج متطابقة بشكل جيد .

List of symbols

$\{A\}$ magnetic vector potential vector
$\{B\}$ magnetic flux density vector
$\{D\}$ electric flux density vector
$\{E\}$ electric field intensity vector
$\{H\}$ magnetic field intensity vector
$\{J\}$ total current density vector
$\{J_c\}$ applied source current density vector
L_{Fe} core length of machine
r radius
S surface of integration
t time
T_e electromagnetic torque
σ Maxwell stress tenser
$\mu_\circ$ permeability of free-space
[ν] reluctivity matrix $= \frac{1}{[\mu]}$
[σ] conductivity matrix
$\vee$ electric scalar potential
$\nabla\times$ curl operator
$\nabla\cdot$ divergence operator

1. Introduction

Single-phase induction motors (SPIM) operating from single-phase supplies and they are mostly designed for fractional horsepower range.

These motors are widely used in industrial and household applications. To obtain starting torque, there is typically an auxiliary winding displaced in phase position from the main winding, the auxiliary winding usually has fewer turns than the main winding. Sometimes there is a capacitor in series with this auxiliary winding for motor starting and to improve the efficiency at the steady-state. Once started by auxiliary means, the motor will continue to run. The analysis of the SPIM is based on the knowledge of the magnetic field in the machine.

The Finite Element Method (FEM) is recognized nowadays as a powerful numerical method for evaluation of magnetic field problems in electromagnetic machines and devices, in which material nonlinearities and

complicated geometric shapes are often encountered.

Kudla was investigated the field-circuit models of induction motor at transient state, and compared the results with circuit models. He found that the circuit models were more suitable for simulation of the motor. **Lombard et al** are presented a generalized formulation for direct coupling 2-D FE analysis with massive and stranded conductors using sinusoidal voltage source. The method was applied to induction motor with squirrel-cage rotor at locked rotor coupling with external circuit. They gave the computational results and the measurements of the currents in the three-phase and for the torque at the starting state.

In this work the single-phase capacitor motor is analyzed using 2-D FEM at locked-rotor condition, also the effect of changing capacitance motor on the parameter is studied. The computed results are compared with experimental results and found a good agreement between them.

2. Calculation Method

The single-phase capacitor motor is treated as quasi-static magnetic system, so the magnetic field is governed by Maxwell's equations, as follows [3]:

$$\nabla \times \{H\} = \{J\} \qquad (1)$$

$$\nabla \times \{E\} = -\left\{\frac{\partial B}{\partial t}\right\} \qquad (2)$$

The constitutive relations applicable to the field problem are given by

$$\{H\} = [\upsilon]\{B\} \qquad (3)$$

$$\{J\} = [\sigma]\{E\} \qquad (4)$$

$$\nabla \cdot \{B\} = 0 \qquad (5)$$

The magnetic vector potential $\{A\}$ and the magnetic flux density $\{B\}$ are related as:

$$\{B\} = \nabla \times \{A\} \qquad (6)$$

And the electric field $\{E\}$ can be expressed as

$$\{E\} = -\left\{\frac{\partial A}{\partial t}\right\} - \nabla V \qquad (7)$$

The displacement currents are assumed to be small compared to the conductive currents in the conductors, i.e.

$$J = J_c + \frac{\partial D}{\partial t} \qquad (8)$$

But $\frac{\partial D}{\partial t} << J_c$

Then $J = J_c$

We get the equations for the vector and scalar potentials [4]

$$\nabla \times [\nu] \nabla \times \{A\} = \{J\} \qquad (9)$$

Equation (9) is reduced for the two-dimensional (2-D) problem to the well-known Poisson's equation, where the magnetic vector potential and current density have only z-axis components and their values are determined in the x y – plane [5]:

$$\frac{\partial}{\partial x}\left(\nu \frac{\partial \mathrm{A}z}{\partial x}\right) + \frac{\partial}{\partial y}\left(\nu \frac{\partial \mathrm{A}z}{\partial y}\right) = -J \qquad (10)$$

This is called the Poisson's equation. It describes the magnetic field when a planar case with a perpendicular current carrying conductor is considered. The method used for computation is Finite Element Method (FEM) in 2-D. Based on these equations, a finite element software package (ANSYS V.8) was used. The magnetic vector potential is solved in the core region and air-gap of the motor using the above software [6].

The two-stator windings for the single-phase induction motor are shown in Fig.(1). The model used for computation as well as the finite element mesh is shown in Fig. 2. The machine geometry repeats itself after 120° of the model circumference.

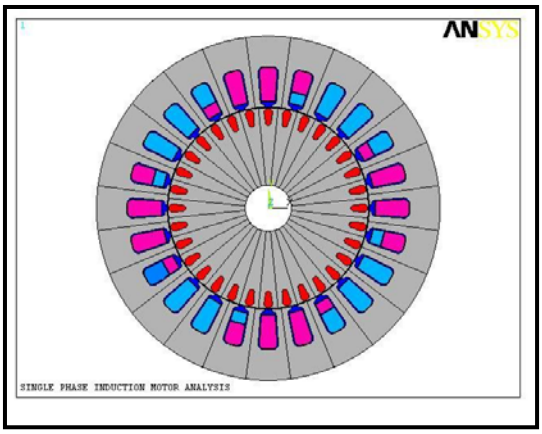

Fig.1 Model of the 2-D SPIM cross section
Main winding
Auxiliary winding

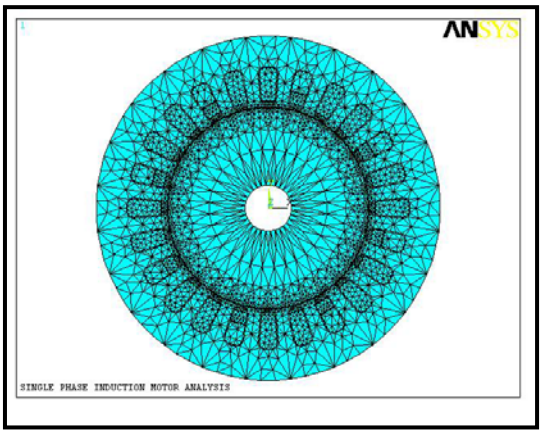

Fig. 2 FE Model of SPIM section

3. Torque Calculation

The electromagnetic torque depends on the accurate evaluation of the air-gap flux density components. The Maxwell's stress tensor can be applied to a closed surface around the iron. Here the surface is chosen in the air-gap closed surface. The basics of this method are to compute the torque at any surface that encloses rotor, such as air-gap. The electromagnetic torque is obtained as a surface integral [7]:

$$T_e = \oint_s r \times \sigma . ds \qquad \ldots.(11)$$

Where σ is Maxwell's stress tensor, s is the surface of integration which is taken to be cylindrical, radius r is taken midway between the stator and the rotor elements to enclose the rotor. When equation (11) is applied to the calculation of the torque, a closed integration surface that surrounds the rotor in free space must be chosen. In 2-D model the surface integral is reduced to a line integral along the air-gap. If a circle of radius r taken as the integration path, the torque is obtained from the equation [8].

$$T_e = \frac{l_{Fe}}{\mu_o} \int_0^{2\pi} r^2 B_r B_\phi d\phi \qquad \ldots.(12)$$

Where B_r and B_ϕ are the radial-and tangential-components of the flux density, and l_{Fe} being the equivalent core length of the machine. By integration of equation (12) in the radial direction over the air-gap, the electromagnetic torque is [8]:

$$T_e(r_s - r_r) == \frac{l_{Fe}}{\mu_o} \int_{S_{ag}} r B_r B_\phi ds \qquad \ldots. (13)$$

Where r_s and r_r are the outer and inner radii of the air-gap respectively, and S_{ag} is the cross sectional area of the air-gap.

4. Simulation Results

The parameters of the analyzed capacitor motor are given in Table 1. [9]
The locked- rotor condition is one of the operation states which is used to analyze the single-phase capacitor motor by numerical field solution methods.
In this case there is no need to take the motion into account, so the slip is one $(s = 1)$. The stator iron is supposed to carry no induced currents as it is laminated. However, the rotor is at standstill and currents are induced in bar at slip frequency. The magnetic and electrical parameters, such as stator currents and torque are calculated in each time step. When the winding currents and torque reach their stable values after a number of cycles, the average torque and RMS currents in the last cycle wave would be obtained.

Rated power	1/4 h.p.
Rated Voltage	220V
Rated Frequency	50 Hz
Number of pole	4
Number of Stator Slot	24
Number of Rotor bars	32

Table 1: parameters of motor

Table (2) shows simulated RMS current in each winding and the starting torque for locked-rotor. It can be seen that the values computed by (ANSYS V.8) using F.E. method are well matched with the measured results.

Table (2) the comparison between locked-rotor characteristics obtained by the finite-element method and experimental method.

No.	Item	Locked-rotor		Error %
		Computed	experimental	
1	Current main (Amp.)	2.48	2.4	3.2
2	Current aux. (Amp.)	0.51	0.48	5.8
3	Starting torque (N.m)	0.65	0.62	4.6

Fig (3) shows the distribution of flux lines in the capacitor motor at start up.
At this time, all flux lines are concentrated at the surface of the rotor because at standstill the rotor current flows only in part of the cross-section of the rotor bars, the rotor resistance appears high, the total flux across the bars is reduced which causes a reduction in the rotor reactance. This variation of the rotor bar resistance and reactance is known as deep-bar (or skin effect). The leakage reactance at locked-rotor is smaller than its value at full load, a main cause of the reduction at starting is magnetic saturation of the stator and rotor tooth tips due to the combined effects of zigzag and slot-leakage flux.

Fig (4) shows the time variations of the stator currents (main and auxiliary) vary sinusoidally with time. A large fluctuation in main current and a small fluctuation in auxiliary current are found. The main difference between the two waveforms is the distortion in the auxiliary winding current.

Fig (5) shows the time variation of torque at locked-rotor. The torque is calculated at each time step, and as a result one gets the torque as a function of time. In the first few moments, the torque shows large oscillation but after about (0.3 sec) it's mean value can be considered constant and equal to its steady-state value.
Also Fig (6) shows the emf waveforms of the main and auxiliary winding. It can be seen that the auxiliary emf lags the current by 90°. The reason is that the current can be considered as the current passing through the capacitor. The main winding waveforms of current and emf are very close to sinusoidal waveforms.

5. Effect of Motor Capacitor on the Starting Performance

In order to show the flexibility of the simulation on motor design the auxiliary branch capacitor changed in step of $2\mu F$ (increasing and decreasing). So the values for auxiliary winding capacitor taken as ($2\mu F, 4\mu F, 6\mu F, 10\mu F, 12\mu F$) and the effect of each case studied on the starting performance of the motor.
Table (3) explains the achieved results while Fig. 7, 8 shows there for c= 2μF, and Figs 9, 10 shows the effect on I_{st} and T_{st} at 12μF. These results show that the auxiliary current increased with the capacitor so as the starting torque. These results confirm the ability of the simulation on finding the performance of the machine when its elements changed. The variation of the capacitor value up to $12\mu F$ is limited by the auxiliary current. In this value ($I_{aux} = 0.89A\ rms$) which is about ($1.5 I_{auxrated}$). This result can be

considered as a recommendation to the manufacturer ($I_r = 1.2A.$).

In Fig.4 and Fig.9 we show that the increase in capacitor value from ($8\mu F$) to ($12\mu F$) will lead to increase the value of the auxiliary current because the capacitor is connected in series with the auxiliary winding. So, the waveform of the auxiliary current in Fig.9 will be more sooth than the waveform of the auxiliary current in Fig.4, but this increase will lead to increase in temperature, losses, and will case decrees the efficiency of the motor. In the same way, in Fig.5 and Fig.10 the starting torque (T_{st}) will increase with increased the value of the capacitor from ($8\mu F$) to ($12\mu F$).

Table (3) the relationship between the capacitor values and the stator currents and starting torque at loaded condition.

Capacitor Value	I_{main} (rms)Amp.	$I_{aux.}$ (rms)Amp.	T_{st} N.m
2 μF	3.25	0.14	0.27
4 μF	3.25	0.32	0.32
6 μF	3.25	0.47	0.47
8 μF	3.25	0.61	0.61
10 μF	3.25	0.75	0.75
12 μF	3.25	0.89	0.89

6. Conclusions

This work concerns with many conclusions can be abbreviated as follows

1. The numerical model using (2-D) FEM for this type of induction motor gives an accurate determination of the motor performance, and can expect the behavior of the motor when the auxiliary capacitor values changed. This means that this software package can be used to study the effect of other changes in machine construction parameters, like dimensions, type of material, gauge of wire, etc.
2. The obtained results give a clear distribution of flux, flux density, current waveforms, etc. Such results can not be obtained by analytical methods, and this will help to study the effect of slotting on space harmonic distribution, and the effect of current harmonic and torque harmonic on machine performance.
3. Design optimization of any single phase motor (capacitor type) designed can be done using this package.
4. Design of any suggested performance for this type of motor can be performed without the need to traditionally costly and tedious prototypes.

7. References

[1] Kudla, Jerzy, "Simulation Investigations of Induction Motor Start-Up When Using Field-Circuit Model", www.ansoft.com/news/articles/0209_ISEM 2002.pdf.

[2] Lombard, P. and Meunier, G., "A General Method for Electric and Magnetic Coupled Problem in 2D and Magnetodynamic Domain", IEEE. Transactions on Magnetics, Vol.28, No.2, March 1992.

[3] Sadiku, Matthew N.O., Elements of Electromagnetics, third Edition, Oxford University Press, Inc., New York, 2001.

[4] ANSYS Theory Reference, "Electromagnetic Field Fundamentals", ANSYS, V.8, 2007.

[5] Chari, M.V.K. and Silvester, P.P., Finite Elements in Electrical and Magnetic Field problems, John Wiley and Sons, Ltd. New York, 1980.

[6] ANSYS Electromagnetic Field Analysis Guide. Emag, ANSYS, http://www.ansys.com.2006.

[7] Saitz, J., "Magnetic Field Analysis of Electric Machines Taking Ferromagnetic Hysteresis into Account", PhD Thesis, Helsinki University of Technology, Acta Polytechnica Scandinavica, Electrical Engineering Series, No.107, Finland, 2001.

[8] Arkkio, A., "Analysis of Induction Motors based on the Numerical Solution of the Magnetic Field and Circuit Equations", PhD Thesis, Helsinki University of Technology, Acta Polytechnica Scandinavica, Electrical Engineering Series, No.59, Finland, 1987.

[9] State Company for Electric Industries /Baghdad-Iraq

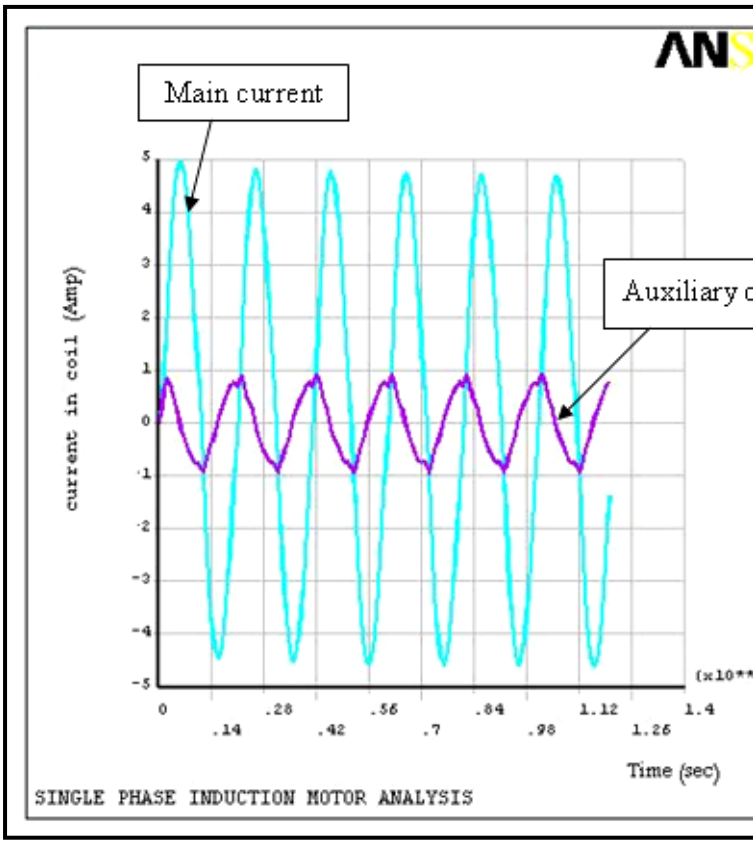

Fig (4) Staring main and auxiliary current versus time at

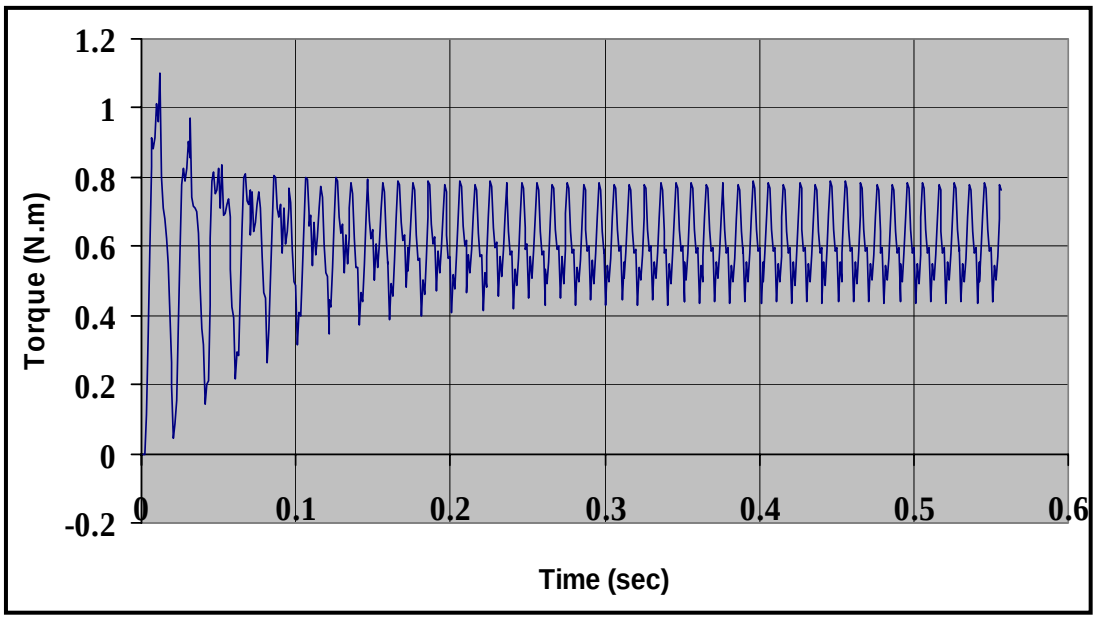

Fig (5) Starting torque versus time at ($8\mu F$)

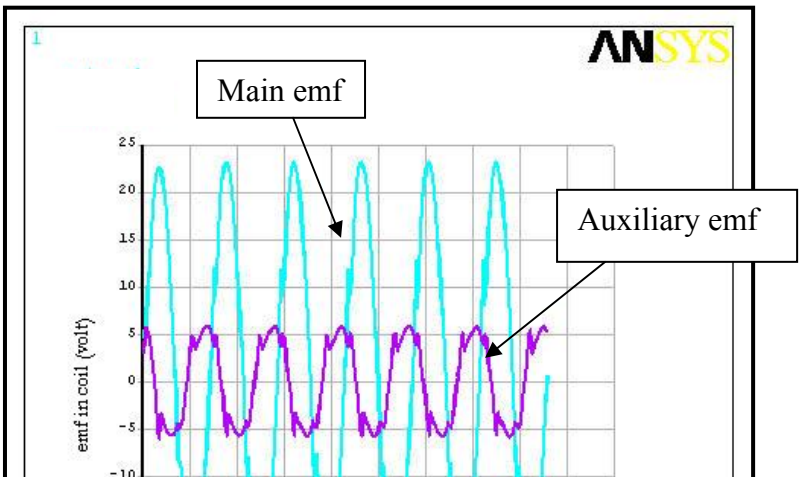

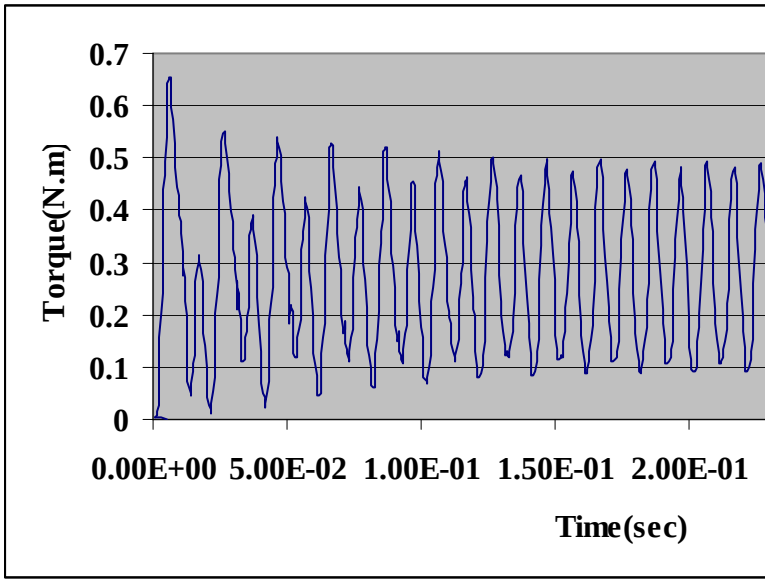

Fig. (8) the variation of starting torque with time at locked

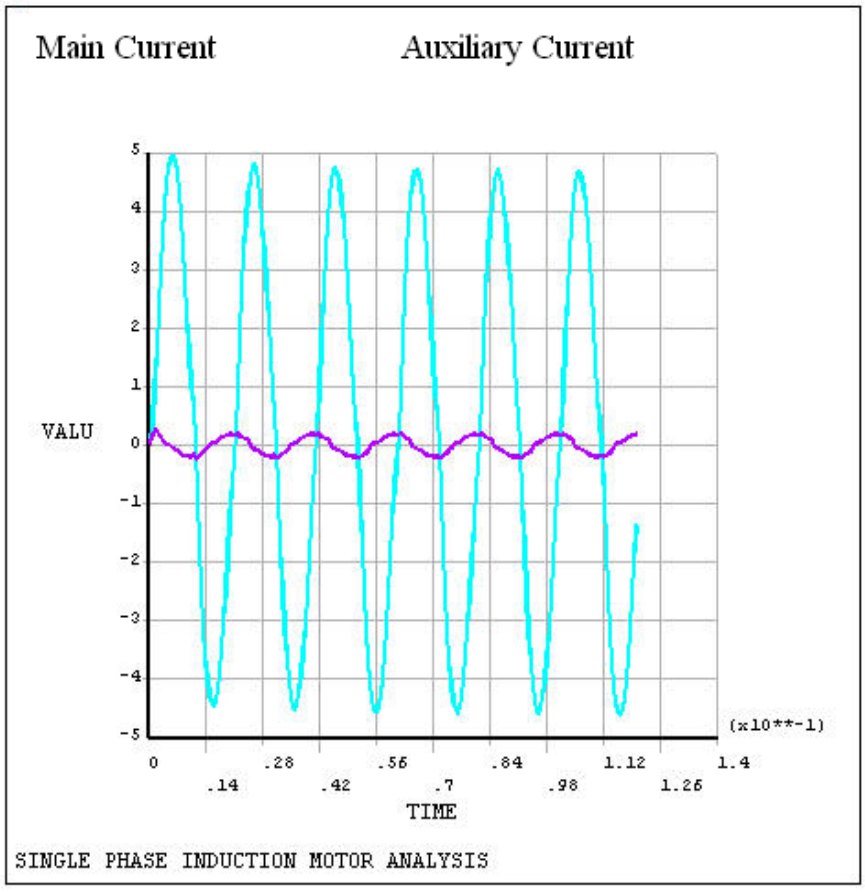

Fig (7) The variation of starting currents with time at locked-rotor condition at 2μF

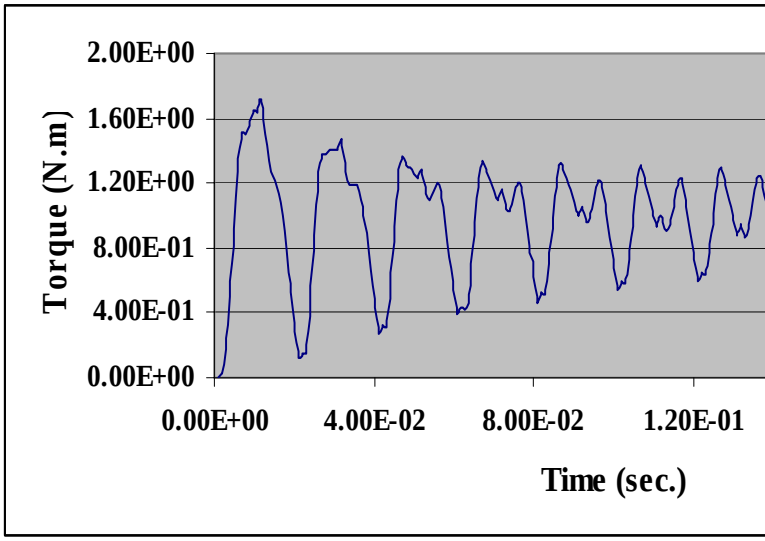

Fig. (10) the variation of starting torque with time at loc

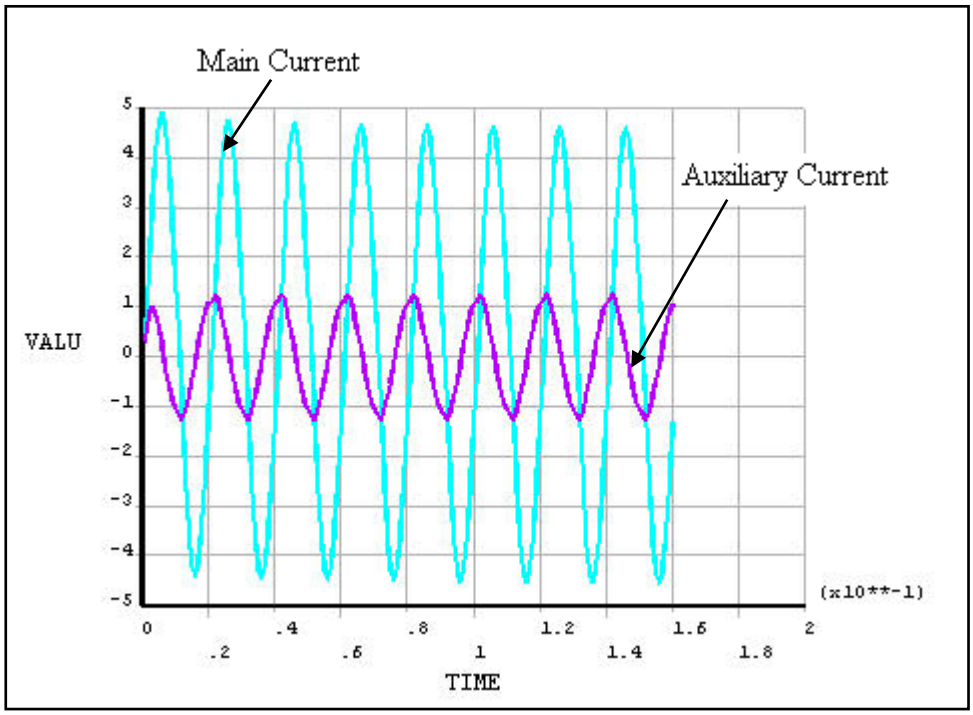

Fig (9) The variation of starting currents with time at locked-rotor condition at 12 µF

7. References

[1] Kudla, Jerzy, "Simulation Investigations of Induction Motor Start-Up When Using Field-Circuit Model", www.ansoft.com/news/articles/0209_IS EM 2002.pdf.

[2] Lombard, P. and Meunier, G., "A General Method for Electric and Magnetic Coupled Problem in 2D and Magnetodynamic Domain", IEEE. Transactions on Magnetics, Vol.28, No.2, March 1992.

[3] Sadiku, Matthew N.O., Elements of Electromagnetics, third Edition, Oxford University Press, Inc., New York, 2001.

[4] ANSYS Theory Reference, "Electromagnetic Field Fundamentals", ANSYS, V.8, 2007.

[5] Chari, M.V.K. and Silvester, P.P., Finite Elements in Electrical and Magnetic Field problems, John Wiley and Sons, Ltd. New York, 1980.

[6] ANSYS Electromagnetic Field Analysis Guide. Emag, ANSYS, http://www.ansys.com.2006.

[7] Saitz, J., "Magnetic Field Analysis of Electric Machines Taking Ferromagnetic Hysteresis into Account", PhD Thesis, Helsinki University of Technology, Acta Polytechnica Scandinavica, Electrical Engineering Series, No.107, Finland, 2001.

[8] Arkkio, A., "Analysis of Induction Motors based on the Numerical Solution of the Magnetic Field and Circuit Equations", PhD Thesis, Helsinki University of Technology, Acta Polytechnica Scandinavica, Electrical Engineering Series, No.59, Finland, 1987.

[9] State Company for Electric Industries /Baghdad-Iraq